ELSEVIER

International Journal of Biological Macromolecules 42 (2008) 271–277

INTERNATIONAL JOURNAL OF
Biological
Macromolecules
STRUCTURE, FUNCTION AND INTERACTIONS

www.elsevier.com/locate/ijbiomac

A hydrophobic loop in acyl-CoA binding protein is functionally important for binding to palmitoyl-coenzyme A: A molecular dynamics study

Diego F.G. Vallejo [a,b], J. Raúl Grigera [a,c], Marcelo D. Costabel [d,*]

[a] *Instituto de Física de Líquidos y Sistemas Biológicos (IFLYSIB), UNLP-CONICET-CIC, Argentina*
[b] *Facultad de Ingeniería, Universidad Nacional de La Plata, Argentina*
[c] *Departamento de Ciencias Biológicas, Facultad de Ciencias Exactas, Universidad Nacional de La Plata, Argentina*
[d] *Grupo de Biofísica, Departamento de Física, Universidad Nacional del Sur, Av. Alem 1253, 8000 Bahia Blanca, Bs. As., Argentina*

Received 30 June 2006; received in revised form 8 December 2007; accepted 10 December 2007
Available online 23 December 2007

Abstract

Acyl-CoA binding protein (ACBP) plays a key role in lipid metabolism, interacting via a partly unknown mechanism with high affinity with long chain fatty acyl-CoAs (LCFA-CoAs). At present there is no study of the microscopic way ligand binding is accomplished. We analyzed this process by molecular dynamics (MDs) simulations. We proposed a computational model of ligand, able to reproduce some evidence from nuclear magnetic resonance (NMR) data, quantitative time resolved fluorometry and X-ray crystallography. We found that a hydrophobic loop, not in the active site, is important for function. Besides, multiple sequence alignment shows hydrophobicity (and not the residues itselves) conservation.

Keywords: Acyl-coenzyme A binding protein; Long chain fatty acyl-coenzyme A; Molecular dynamics; Lipid protein interactions; Hydrophobic interaction

1. Introduction

Disorders of fatty acid oxidation are linked to metabolic decompensation, hypoketotic hypoglycemia, and acute dysfunction of fatty acid-dependent tissues [1]. Long chain fatty acyl-CoAs (LCFA-CoAs) are part of the oxidation process, (also they have other physiological functions like fatty acid esterification, signal transduction, gene regulation and membrane trafficking) [2,3] (and refs therein). Oxidation occurs mainly in mitochondria, after crossing the cell membrane; also, defects in LCFA-CoAs transport are associated with acute liver failure [1].

It follows that regulation of the level and intracellular targeting of LCFA-CoAs becomes important to maintain cell functions. Acyl-CoA binding protein (ACBP), a highly conserved and widely distributed 10 kDa cytosolic protein, has here a central role: binds C_{12}–C_{22} LCFA-CoAs with high affinity and specificity ($K_d \sim 0.1$ nM) [2,3]. Besides, ACBP specifically mediates reactions like removing, storing, transporting and donating LCFA-CoAs from/to membranes [2,4].

ACBP consists of 86–103 amino acids, which fold into a four α-helix bundle forming a shallow bowl-like structure with a binding pocket for LCFA-CoAs [3]. Three-dimensional structures are available: NMR of bovine ACBP complexed with palmitoyl-CoA (from Protein Data Bank [5], accession no. 1NVL[1]), X-ray bovine [6] (PDB accession no. 1HB8) and X-Ray Armadillo Harderian Gland ACBP (HgACBP) [7] (PDB accession no. 2FDQ).

In spite of the efforts, the molecular mechanism involved in binding remains poorly understood [8]. Our purpose here was to simulate/analyze the association of ACBP with a typical LCFA-CoA: palmitoyl-CoA (PlyCoA), reporting the first molecular dynamics (MDs) study of a ligand binding with ACBP. More-

Abbreviations: LCFA-CoA, long chain fatty acyl-CoA; CoA, coenzyme A; ACBP, acyl-CoA binding protein; HgACBP, armadillo harderian gland ACBP; PlyCoA, palmitoyl CoA; NMR, nuclear magnetic resonance; MDs, molecular dynamics; SASA, solvent accessible surface area; RMSF, root mean square fluctuations.

* Corresponding author. Tel.: +54 291 4595101; fax: +54 291 4595142.
E-mail address: costabel@criba.edu.ar (M.D. Costabel).

[1] M.H. Lerche, B.B. Kragelund, C. Redfield, F.M. Poulsen, Rdc-refined NMR structure of bovine acyl-coenzyme A binding protein, ACBP, in complex with palmitoyl-coenzyme A, 2003 (unpublished data). We will refer to this structure as 1NVL in what follows.

0141-8130/$ – see front matter © 2007 Elsevier B.V. All rights reserved.
doi:10.1016/j.ijbiomac.2007.12.003

over, we performed a MDs with native and mutant HgACBP, showing the relevance of a hydrophobic loop in the interaction process.

2. Models and methods

MDs simulations were performed with GROMACS [9], using the GROMOS96 43A1 force field [10]. Simulations utilized the NPT ensemble with pressure coupling ($\tau_p = 0.5$ ps) to 1 bar and temperature coupling ($\tau_T = 0.1$ ps) to 300 K. Berendsen coupling schemes were used for both pressure and temperature [11]. Long-range electrostatics were computed with a 0.9 nm cut-off, using the particle mesh Ewald (PME) method [12]. Van der Waals interactions were cut-off at 1.4 nm, bond lengths were constrained with LINCS [13] and water geometries with SETTLE [14]. SPC/E [15] was the water model and no artificial ad hoc forces, like 'pull springs' or steered procedures drove binding.

The setup of the simulation system consist in one chain (86 amino acids) from HgACBP structure (PDB code 2FDQ) [7] and one molecule of PlyCoA, extracted manually from the complex structure (PDB code 1NVL).

Initially, the protein was protonated with PDB2PQR [16] and the total ACBP charge was zero. After that, 19 minimizing steps were performed without solvent. The protein was solvated in a 5.0 nm × 5.4 nm × 5.2 nm box with 4184 water molecules without counter ions added. We energy minimized again and a 400 ps run with velocities resignation was performed.

Separately, we extracted manually ligand coordinates from structure no. 1 from 1NVL and built the topology of PlyCoA by inspecting similar structures in the force field with focus on consistency. Total charge of model was −4 and four water molecules were replaced with Na^+ counter ions to achieve electroneutrality. Then, a 1.25 ns run was performed for stabilize the ligand structure. The final model is schematically depicted in Fig. 1.

Finally, we assemble the protein + ligand + $4Na^+$ + water system, with VMD [17]. PlyCoA was placed according our previous work[2] and data from literature [8], and the PlyCoA–ACBP distance was set to 1.0 nm, from closest van der Waals surfaces.

Again, the whole structure was minimized-solvated-minimized in a 200 ps MDs run and stabilization of the potential energy was monitored as first equilibrium criterium. With the same procedure, we built five more samples (m1, m2, m3, m4 and m5), with different ligand starting points, surrounding the ACBP. Fig. 2 shows the initial position for the different runs. H-bonds autocorrelation function for bulk water agreed with literature [18] showing solvent equilibrium (H-bonds were determined geometrically with a distance cut-off of 3.5 Å and angle cut-off of 60°). Analyses were primarily performed using tools in the GROMACS suite: solvent accessible surface area (SASA) was computed with *g_sas* [19], and root mean square fluctuations (RMSF) with *g_rmsf*. Hydrodynamic radius was computed with Hydropro [20]. Molecular graphics were rendered using VMD [17] and Gnuplot (T. Williams, W. Kelley et al., v4. http://www.gnuplot.info/). Planar interaction graphics were produced with LigPlot [21].

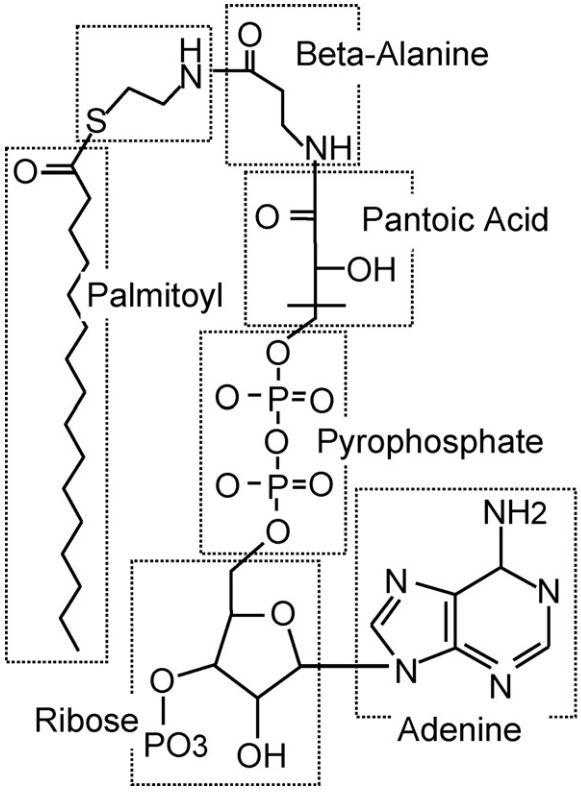

Fig. 1. Palmitoyl-CoA block model, used to build the atomistic model for the simulations.

To confirm the structural importance of three hydrophobic conserved positions (Met46–Leu47–Phe49) localized in the loop between helix 2 and helix 3, we carried out simulations of a mutant HgACBP. The mutations were Met46Asn–Leu47Asn–Phe49His, maintaining similar structure but lowering the hydrophobicity. The simulation was carried out in the same way described above.

3. Results

Only the 'm0' sample showed binding; none of the rest of the samples converged to a complex. What follows is the m0 sample results. We monitored distance between the respective molecules' center of masses vs. time, and we observed that PlyCoA were approaching to ACBP (not shown). After 1 ns the ligand came into contact with the protein. We tried to evaluate how close comes our data compared to the 1NVL structure. In order to do so, we analyzed the 20 NMR models in the 1NVL file and selected eight atom pairs (one in the ligand and the other in the protein). Then, we compared the interatomic distance versus the NMR distribution of distances for each pair. Fig. 3A and B shows this comparison for two such pairs vs. time. We see that first the carbon CG of PlyCoA makes contact with ACBP (Oxygen Phe49.O) in the first nanosecond. At $t \approx 9$ ns the sulphur PS1 does the same. Fig. 4 shows a LigPlot drawing of the initial interaction based on our MDs simulation ($t = 965$ ps snapshot).

[2] D.F. Vallejo, J.R. Grigera, M.D. Costabel, unpublished work.

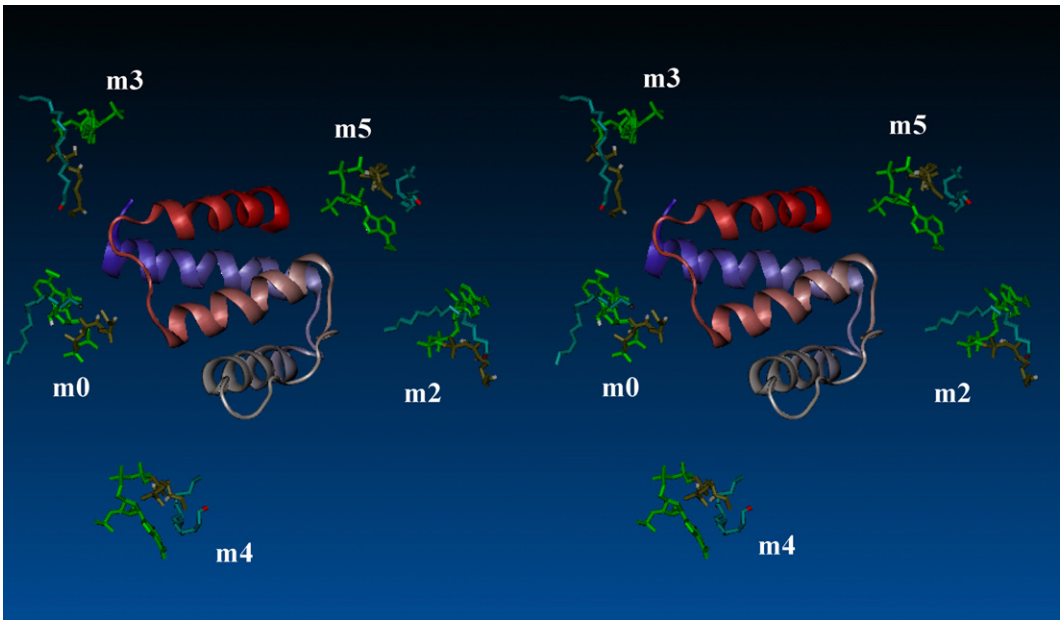

Fig. 2. Stereo view of ACBP–PlyCoA complex. The figure shows the ligand positions for each initial configurations used in the molecular dynamics carried out. The initial position in each case is arbitrary and the different positions surrounded the protein were labeled m0, m2, m3, m4 and m5. Only the m0 sample converged to a complex.

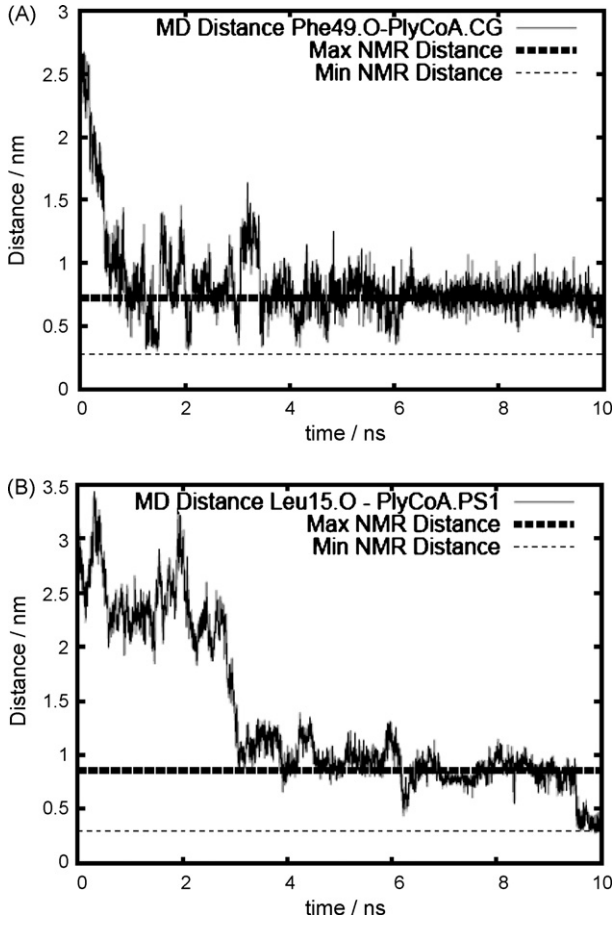

Fig. 3. Time dependent distance between selected atoms from ACBP and the ligand PlyCoA A) distance between Phe49 oxygen and PlyCoA-CG B) Leu15 oxygen–carbon PlyCoA-CG distance vs. time. Dashed lines: maximum (bold) and minimum (thin) of distance according to 1NVL NMR data.

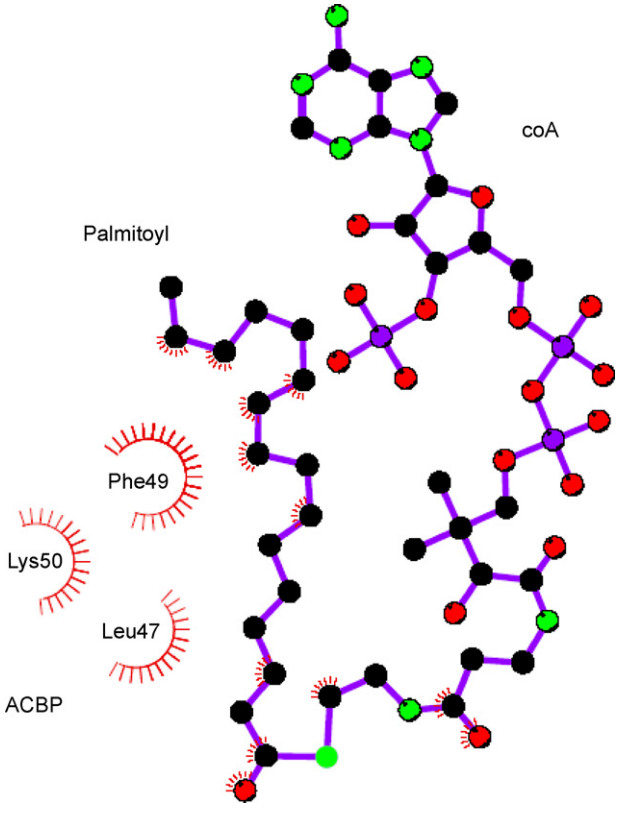

Fig. 4. Planar graph of MDs snapshot of ACBP–PlyCoA complex at $t = 965$ ps showing protein–ligand interactions. The red rays show the groups and atoms involved in the interaction. (For interpretation of the references to colour in this figure legend, the reader is referred to the web version of the article.)

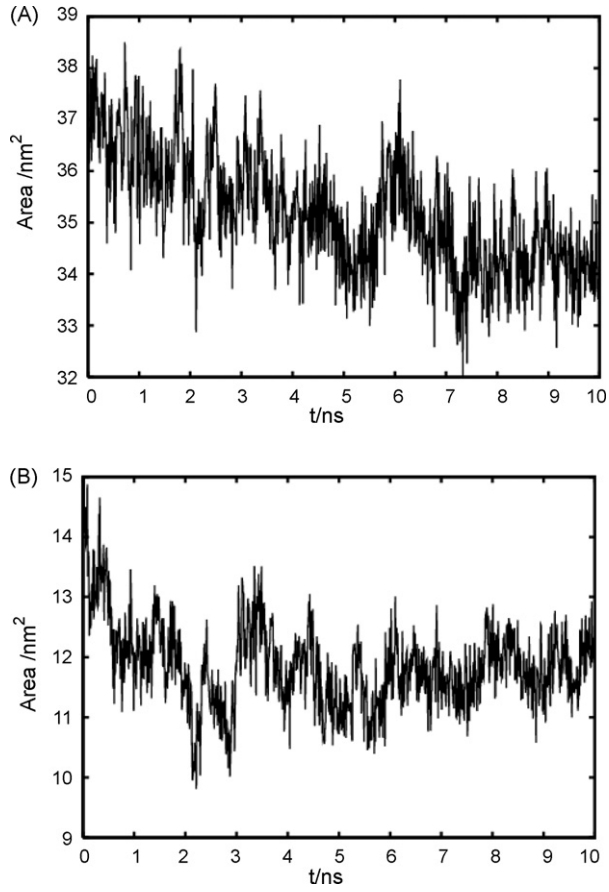

Fig. 5. Time dependent graphics showing the solvent accessible surface area (SASA). (A) Hydrophilic area vs. time and (B) hydrophobic area vs. time. Note the different scales in the vertical axis. The SASA (both polar and nonpolar) decrease is consistent with the amphiphilic nature of ligand; moreover, nonpolar SASA shows initial decrease and later stabilization reinforcing the idea of hydrophobic interaction acting mainly in the initial recognition.

Additionally, the solvent accessible surface area (SASA) was analyzed. Total ACBP–PlyCoA SASA decreases on binding (not shown) and the ligand exposed area variation was negative ($-5.7\,\mathrm{nm}^2$) in the first 7 ns. We see that both, hydrophobic and polar SASA, decrease (Fig. 5A and B). In the hydrophobic case the effect appears only in the first 1–2 ns, and then arrives to a plateau. We proceeded to split this area into per-residue contributions. According to its time evolution we classified the amino acids in: (I) *residues that increment area*: these are 61, 64, 68 and 83. Initial areas are consistent with the hydrophobic type of Leu61 ($A_{61} \approx 0.4\,\mathrm{nm}^2$) and hydrophilic type of Lys83 and Asp68 ($A_{83} \approx 1\,\mathrm{nm}^2$ and $A_{68} \approx 0.6\,\mathrm{nm}^2$ such that $A_{61} < A_{83}, A_{68}$). These amino acids are located in helix α4, in the loop between 3rd and 4th (Leu61). Notably, they are on the opposite side of the union zone with the ligand. (II) *Variable area residues*: residues 46, 47 and 49 decrease and later increment (in 4 ns) their area to the starting value (Fig. 6). These are strongly exposed to water, in spite of being hydrophobic and they belong, notably, to the first zone making contact with PlyCoA. Also note that Leu47 lowers its area first, and then Met46 and Phe49 do the same. This suggests that the three act as a "hydrophobic signal" to attract the ligand, being Leu47 the 'first step'. After the initial contact, the

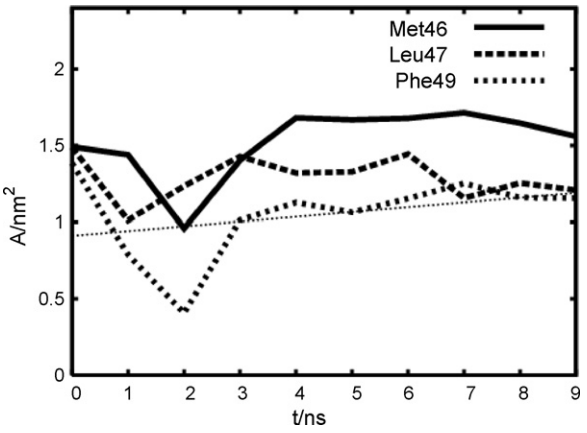

Fig. 6. Exposed area of residues Met46, Leu47 and Phe49 vs. time. The area decrease and later increment (in 4 ns) to the starting value showing the initial contact with the ligand. The finely dotted line is a lineal regression for the data, showing the increasing character of them.

ligand should move on the surface of ACBP until it reaches its final place according to 1NVL NMR data. (III) *Area decreasing residues*: the fitted line slope to the area versus time allows us to further find the most significant amino acids. So Lys18 and Lys50 (hydrophilic) and Met24 (hydrophobic) are the three with most important variations. Their areas are: $A_{18} \approx 1.5\,\mathrm{nm}^2$ and $A_{50} \approx 1.3\,\mathrm{nm}^2$, greater than $A_{24} \approx 0.7\,\mathrm{nm}^2$. They are implicated in the interaction with the ligand in the 1NVL structure these three amino acids are coordinated with PlyCoA. This can also be seen in the simulation.

Further validation was obtained when we computed the time evolution of hydrodynamic radius. A tightening of the structure of bovACBP when binding was reported [3] and time resolved fluorometry data for the binding of rat liver ACBP with oleoyl-CoA, shows a 0.2 nm decrease of ACBP hydrodynamic diameter [22]. Being the experimental system similar to ours, we qualitatively reproduce the trend (Fig. 7). The initial increase of radius is due to incorporation of ligand to the calculation. The radius could further decrease beyond last step shown.

Also we computed the RMSF fluctuations for ACBP without ligand. In this case we found agreement with 1HB8 B-factors

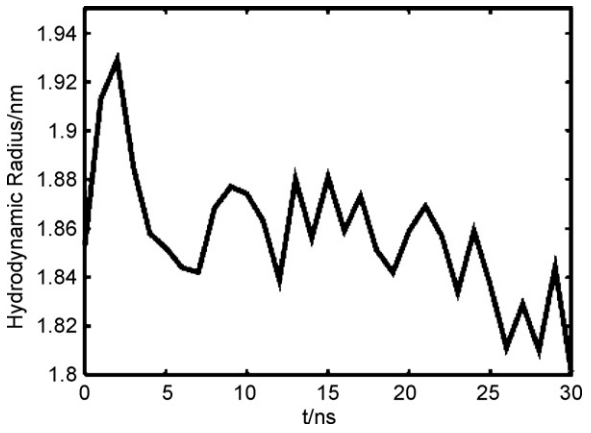

Fig. 7. The figure shows the time evolution of the computed hydrodynamic radius. This data reproduces the trends in Ref. [22].

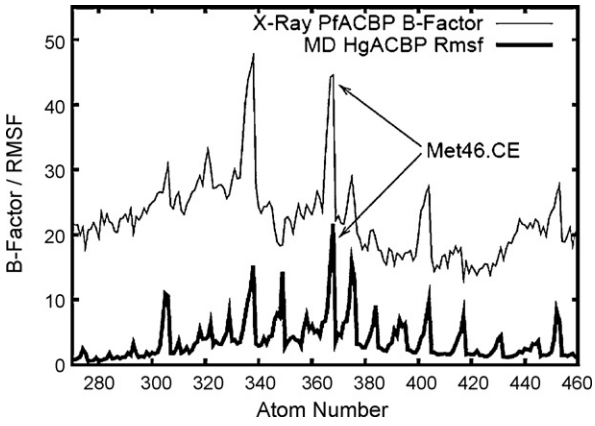

Fig. 8. X-ray structure B-factors (1HB8 structure) vs. computed RMSF (MDs of HgACBP). In both cases the Met46 shows a shaky behavior.

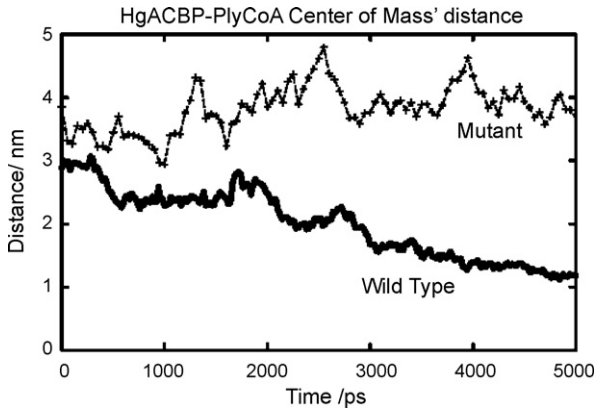

Fig. 10. Time dependent molecular dynamics of mutant (Met46Asn–Leu47Asn–Phe49His) HgACBP. The simulation was carried out for 6 ns and the distance between the mass centers of the protein and the ligand shows no decrease.

(Fig. 8), particularly in Met46, which has one of the most shaky side chain in the structure.

Following [23] we computed the protein–ligand interaction energies, excluding solvent contributions. This can be seen in Fig. 9 and we found that binding is favored initially by Lennard Jones forces, with no electrostatic contribution.

To further justify the argument that the hydrophobic loop has a significant importance in the complex formation, a simulation of HgACBP with Met46Asn–Leu47Asn–Phe49His mutations was performed with the ligand placed in the same initial orientation as m0 configuration. The molecular dynamics was carried out for 6 ns, and the average distance between the mass centers was monitored. This distance showed no sign of approach in this lapse (Fig. 10). Considering that in the native structure the interaction starts in 2 ns, we conclude that the mutations are responsible for this behavior and as a result, the hydrophobic character of the amino acids in that positions is relevant for the complex formation.

4. Discussion

Almost all members of the FABP/P2/CRBP/CRABP protein family of β-barrel lipid binding proteins have hydrophobic side chains that protrude directly into solvent (rather than being directed internally). These, like 'devices' interact with membranes and ligands [24]. Also membrane-binding C2 domains of blood coagulation cofactors Va and VIIIa bind anionic phospholipids through protruding solvent-exposed hydrophobic residues [25]. We recognize a similar mechanism here. The interatomic distance plots (Fig. 3) show that the way PlyCoA enters into ACBP resembles the way it associates with macromolecular complexes, by insertion of the carbon chain as was noted recently by experimental evidence on binding to phospholipid membranes [8], or computational studies of palmitoyl with ALBP [23]. Initial contact is between hydrophobic groups of either molecule (carbon tail of PlyCoA, and residues 46, 47 and 49 of ACBP, Fig. 4). The first contact, the introduction of the PlyCoA-CG in the region, is compatible with experimental data [2]. In Fig. 4, we show schematically the relative position of residues 46, 47 and 49 respect the tail of the ligand, at $t = 965$ ps. Presumably, these residues could orientate ACBP in the protein-membrane interaction[3]. In the next step, between 3 and 5 ns, the sulphur atom of PlyCoA is positioned in the correct place staying in this site throughout simulation and arriving at the minimum distance near the 9 ns (Fig. 3B). In this way the sulphur atom PS1 make and break hydrogen bondings with residues Lys13 and Lys15.

Analysis of the solvent accessible surface area shows that the total SASA decrease (both polar and nonpolar) is consistent with the amphiphilic nature of ligand (Fig. 5A and B); moreover, nonpolar SASA shows initial decrease and later stabilization: this reinforces the idea of hydrophobic interaction acting mainly in the initial recognition. Amino acids are located in the loop between helix α2 and helix α3. Interestingly Met46 has high B-factors in both HgACBP and 1HB8 structures and our RMSF calculations show agreement with these data (Fig. 8), suggesting the mobile character of the side chain.

On the other hand, all the samples where the starting point of the ligand was far from the 46 to 49 residues failed to bind in 6 ns.

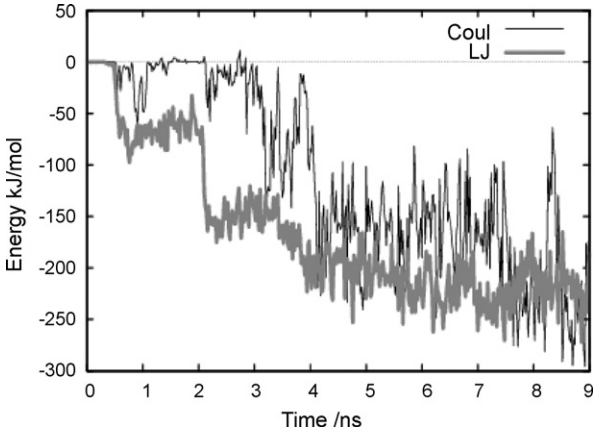

Fig. 9. LJ (thick gray) and Coulomb (thin black) components of protein–ligand interaction energies. In the first 4 ns the LJ interaction is the dominant part.

[3] D.F. Vallejo, J.R. Grigera, M.D. Costabel, unpublished work.

Moreover when we mutated the amino acids as described above and carry out the simulation with the ligand near the loop, the behavior was similar and the PlyCoA does not bind the ACBP molecule. This suggests that ACBP presents this highly mobile 'hook' where, after diffusional encounter, hydrophobicity plays an important role for ligand capture (this loop could also be important for ACBP membrane insertion). Consistent with this, the interaction energies show that the Coulomb component is not the initial driving force for binding (Fig. 9), and LJ part is. This agrees with the findings in Ref. [23] about the hydrophobic nature of adsorption.

We propose that the three exposed residues: Met46–Leu47–Phe49 are a hydrophobic 'hook' tool to initially capture the ligand. Examining a sequence alignment of 30 species, in ref [3], we see that there is no residue conservation in positions 46, 47 and 49, but hydrophobicity do conserve there (100% of species reported in positions 46 and 49 and 90% in 47). Ref. [26] shows that hydrophobicity conservation is required for protein catalytic activity of C-terminal Src kinase. Among FYVE domains, the conserved hydrophobic loop (so-called 'Turret loop') for membrane insertion and phospholipid interaction has also been the focus of attention, showing a general mechanism for membrane entering, anchoring and leaving [27–29]. Although, care must be taken with the generality of this results: a study of the T domain of the diphtheria toxin showed that electrostatic interactions are also fundamental to understand the process of membrane insertion [30]. Besides, it was recently established that ACBP interacts with membranes [4] and that is dependent on membrane content of LCFAs, being ACBP able to extract LCFAs based on hydrophobic interactions [8], connecting binding to membranes and binding to LCFAs. Our calculations, as expected, show that hydrophobic amino acids have less SASA than polar ones (Fig. 5B), exception made for the three residues 46, 47 and 49, much more exposed to water than expected (Fig. 6). In our case, loops 2–3 has never been implicated in the function or in the direct interaction of ACBP with PlyCoA. Nevertheless it plays a role in the biological function of ACBP.

5. Conclusions

Here we have reported the first MDs study of the binding process of ACBP with PlyCoA. A new model of ligand was developed, which is useful for computational simulations analyses. Using this model we were able to reproduce some evidence from NMR data, quantitative time resolved fluorometry, and X-ray crystallography. Careful inspection of simulations have led us to postulate that a loop, mainly of hydrophobic character, not part of the active site, plays a determinant role. This has a good correlation with multiple sequence alignment studies, in the sense that, although there is no residue conservation along the phyla, the hydrophobicity is conserved.

This work has shed some light into the high affinity interaction mechanism of ACBP with LCFA-CoAs. Further studies will be required to analyze subsequent steps of binding, and also the process of sequestering of PlyCoA from a biological membrane.

Acknowledgements

This work has partially been supported by the National Research Council of Argentina (CONICET), the University of La Plata (UNLP), the University of the South (Bahia Blanca) (UNS), the Provincial Research Council of the Province of Buenos Aires (CIC), and one of us (DV). JRG is member of the Carrera del Investigador of CONICET. We thank the SECYT and Vallejo Family for the CPU time. Any of the final structures and intermediate structures that are given in the figures can be obtained in PDB format upon request from one of us.

References

[1] A.A. Odaib, B.L. Shneider, M.J. Bennett, F.R.C. Path, B.R. Pober, M. Reyes-Mugica, A.L. Friedman, F.J. Suchy, P. Rinaldo, N. Engl. J. Med. 339 (1998) 1752–1757.
[2] N.J. Faergeman, J. Knudsen, Biochem. J. 323 (1997) 1–12.
[3] B.B. Kragelund, J. Knudsen, F.M. Poulsen, Biophys. Acta 1441 (1999) 150–161.
[4] H. Chao, G.G. Martin, W.K. Russel, S.D. Waghela, D.H. Russell, F. Schroeder, A.B. Kier, Biochemistry 41 (2002) 10540–10553.
[5] H.M. Berman, J. Westbrook, Z. Feng, G. Gilliland, T.N. Bhat, H. Weissig, I.N. Shindyalov, P.E. Bourne, Nucleic Acids Res. 28 (2000) 235–242.
[6] D.M.F. Van Aalten, K.G. Milne, J.Y. Zou, G.J. Kleywegt, T. Bergfors, M.A.J. Ferguson, J. Knudsen, T.A. Jones, J. Mol. Biol. 309 (2001) 181.
[7] M.D. Costabel, M.R. Ermácora, J.A. Santomé, P.M. Alzari, D.M.A. Guérin, Acta Crystallogr. F 62 (2006) 958–961.
[8] A. Cohen Simonsen, U. Bernchou Jensen, N.J. Faergeman, J. Knudsen, O.G. Mouritsen, FEBS Lett. 552 (2003) 253–258.
[9] E. Lindahl, B. Hess, D. van der Spoel, J. Mol. Mod. 7 (2001) 306–317.
[10] W.F. van Gunsteren, S.R. Billeter, A.A. Eising, P.H. Hünenberger, P. Krüger, A.E. Mark, W.R.P. Scott, I.G. Tironi, Biomolecular Simulation: The GROMOS96 Manual and User Guide, vdf Hochschulverlag AG an der ETH Zürich and BIOMOS b.v., Zürich, Groningen, 1996.
[11] H.J.C. Berendsen, J.P.M. Postman, W.F. van Gunsteren, A. DiNola, J.R. Haak, J. Chem. Phys. 81 (1984) 3684–3690.
[12] T.D. Darden, D. York, L. Pedersen, J. Chem. Phys. 98 (1993) 10089–10092.
[13] B. Hess, H. Bekker, H.J.C. Berendsen, J.G.E.M. Fraaije, J. Comp. Chem. 18 (1997) 1463–1472.
[14] S. Miyamoto, P.A. Kollman, SETTLE: An Analytical Version of the SHAKE and RATTLE Algorithms, 1992.
[15] H.J.C. Berendsen, J.R. Grigera, T.P. Straatsma, J. Phys. Chem. 91 (1987) 6269–6271.
[16] T.J. Dolinsky, J.E. Nielsen, J.A. McCammon, N.A. Baker, Nucleic Acids Res. 32 (2004) W665–W667.
[17] W. Humphrey, A. Dalke, K. Schulten, J. Mol. Graphics 14 (1996) 33–38.
[18] F.W. Starr, J. Nielsen, H.E. Stanley, Phys. Rev. E 62 (1) (2000) 579–587.
[19] F. Eisenhaber, P. Lijnzaad, P. Argos, C. Sander, M. Scharf, J. Comp. Chem. 16 (1995) 273–284.
[20] J. Garcia de la Torre, M.L. Huertas, B. Carrasco, Biophys. J. 78 (2000) 719–730.
[21] A.C. Wallace, R.A. Laskowski, J.M. Thornton, Protein Eng. 8 (1995) 127–134.
[22] A. Frolov, F. Schroeder, J. Biol. Chem. 273 (1998) 11049–11055.
[23] R. Friedman, E. Nachliel, M. Gutman, Biochemistry 44 (2005) 4275–4283.
[24] M.W. Kennedy, J.C. Scott, S. Lo, J. Beauchamp, D.P. Mcmanus, Biochem. J. 349 (2000) 377–384.

[25] J.L. Pellequer, A.J. Gale, E.D. Getzoff, Curr. Biol. 10 (2000) R237–R240.
[26] E. Mikkola, M. Bergman, FEBS Lett. 544 (2003) 11–14.
[27] T.G. Kutateladze, M. Overduin, Science 291 (2001) 1793–1796.
[28] N.R. Blatner, R.V. Stahelin, K. Diraviyam, P.T. Hawkins, W. Hong, D. Murray, W. Cho, J. Biol. Chem. 279 (2004) 53818–53827.
[29] T.G. Kutateladze, D.G.S. Capelluto, C.G. Ferguson, M.L. Cheever, A.G. Kutateladze, G.D. Prestwich, M. Overduin, J. Biol. Chem. 279 (2004) 3050–3057.
[30] A. Chenal, P. Savarin, P. Nizard, F. Guillain, D. Gillet, V. Forge, J. Biol. Chem. 277 (2002) 43425–43432.